dc measurements of macroscopic quantum levels in a superconducting qubit structure with a time-ordered meter

D. S. Crankshaw, K. Segall, D. Nakada, and T. P. Orlando
Department of Electrical Engineering and Computer Science, Massachusetts Institute of Technology, Cambridge, Massachusetts 02139, USA

L. S. Levitov
Department of Physics, Massachusetts Institute of Technology, Cambridge, Massachusetts 02139, USA

S. Lloyd
Department of Mechanical Engineering, Massachusetts Institute of Technology, Cambridge, Massachusetts 02139, USA

S. O. Valenzuela, N. Markovic, and M. Tinkham
Department of Physics, Harvard University, Cambridge, Massachusetts 02138, USA

K. K. Berggren
Massachusetts Institute of Technology Lincoln Laboratory, Lexington, Massachusetts 02420, USA

dc measurements are made in a superconducting, persistent current qubit structure with a time-ordered meter. The persistent-current qubit has a double-well potential, with the two minima corresponding to magnetization states of opposite sign. Macroscopic resonant tunneling between the two wells is observed at values of energy bias that correspond to the positions of the calculated quantum levels. The magnetometer, a superconducting quantum interference device, detects the state of the qubit in a time-ordered fashion, measuring one state before the other. This results in a different meter output depending on the initial state, providing different signatures of the energy levels for each tunneling direction.

PACS number(s): 74.50.+r

I. INTRODUCTION

The study of mesoscopic quantum effects in superconductors is motivated both by interest in the extension of quantum mechanics to the macroscopic world[1] and by the possibility of constructing a quantum information processor.[2] Macroscopic quantum effects, such as resonant tunneling,[3] quantum superposition states,[4,5] and time-dependent coherent oscillations,[4-8] have recently been observed. In these experiments, measurements were made on flux,[4,5] charge,[6] and current.[7,8]

One particular superconducting system that has been under study is the persistent-current qubit (PC qubit), a superconducting ring interrupted by three Josephson junctions.[9] When an external magnetic flux bias near one-half of a flux quantum ($\Phi_0 = h/2e$) is applied, the PC qubit has two stable classical states of electrical current circulating in one direction or the other, resulting in measurable opposing magnetizations. It can be modeled as a double-well potential in a three-dimensional potential landscape (one dimension for each junction's phase variable, or three other variables which span the space), where the minimum of each well corresponds to one of these two magnetization states. Depending on the parameters, the system may have multiple quantum energy levels in one of the two wells, where each level has approximately the same magnetization. Energy levels in a similar system, the radio-frequency superconducting quantum interference device (rf SQUID), have been measured by studying resonant tunneling between the two wells.[3] Experiments on an rf SQUID have used a separate, damped SQUID magnetometer as the meter. This approach gives a continuous readout of the magnetization, but also couples unwanted dissipation into the system.

In a recent paper, we showed how coupling an underdamped dc SQUID magnetometer to a PC qubit resulted in time-ordered measurements of the two states, where one state is observed before the other.[10] In those experiments, we studied the classical, thermally driven regime of operation. In the present paper, we detail the effects of a time-ordered meter on the dc measurements of the PC qubit in the quantum regime. The quantum levels are detected by observing resonant tunneling between the two wells. The positions of the energy levels agree well with calculations of the qubit energy band structure, and the energy bias of level repulsions indicates where tunneling occurs between the two wells. While the PC qubit has inherent symmetry between the two states, the time ordering of the measurements causes an asymmetry in the meter output. We demonstrate this asymmetry, and also show how the meter shifts the positions of the energy levels as a function of the SQUID current bias. Finally, by measuring the width and height of the tunneling peaks as a function of the SQUID ramp rate, we find a fitted value of the intrawell relaxation of order microseconds.

II. QUBIT PARAMETERS AND MEASUREMENT PROCESS

The qubit and dc SQUID are both fabricated at Lincoln Laboratory in a niobium trilayer process.[11] The circuit dia-

(a)

(b)
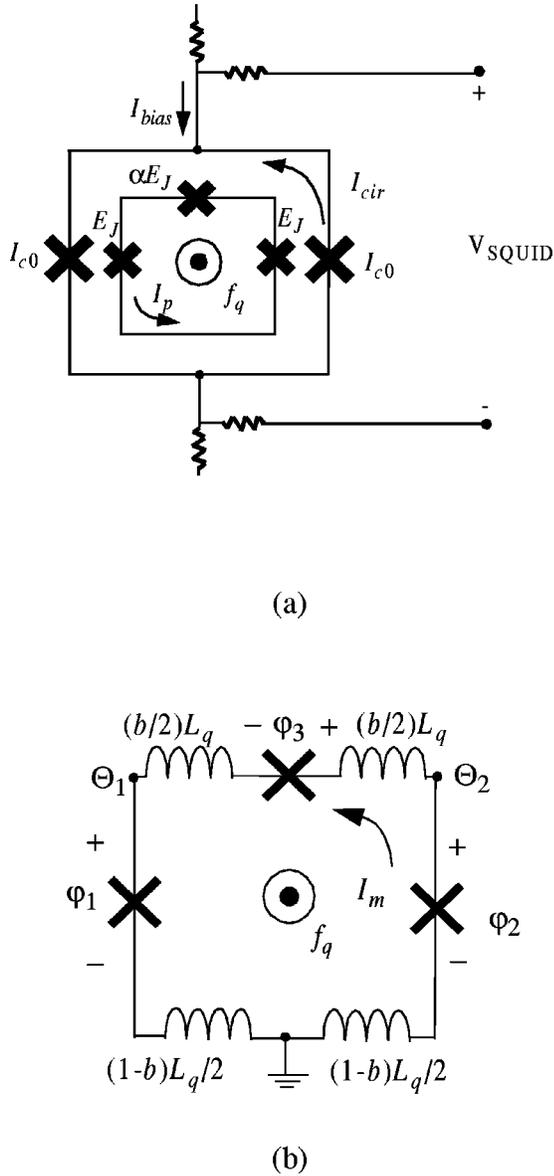
FIG. 1. (a) A circuit diagram of the qubit structure, a three-junction loop, and the two-junction SQUID. (b) The circuit diagram used to derive the quantum-mechanical model of the qubit. The inductance is distributed among the branches, the inductance on the branch of the smallest junction having a value of bL_q (symmetrically split on either side of the junction), while the inductances on the other two branches each have a value of $(1-b)L_q/2$. The node phases Θ_1 and Θ_2 are shown in the figure.

gram is shown in Fig. 1. The qubit consists of a superconducting ring interrupted by three Josephson junctions, two of which are designed to have the same critical current, I_c, and the third of which has a critical current of αI_c, where α is less than 1. The meter is a dc SQUID magnetometer which surrounds the qubit. It has two equal Josephson junctions with critical currents of I_{c0}, where $I_{c0} > I_c$. The PC qubit loop is $16 \times 16~\mu m^2$ in area, and the dc SQUID is $20 \times 20~\mu m^2$ in area, with self-inductances of about $L_q = 30$ pH and $L_s = 60$ pH, respectively. They have a mutual inductance of approximately $M = 25$ pH. These inductances

are calculated using FASTHENRY,[12] then refined through experimental measurements of the SQUID's response to magnetic field, as explained in the Appendix. The critical current density of the junctions is 370 A/cm^2 and the critical current of the SQUID junctions is measured to be $I_{c0} = 5.3~\mu A$, consistent with an area of 1.4 μm^2. I_c and α can be determined experimentally from our previous thermal activation studies, which give $\alpha = 0.63$ and $I_c = 1.2~\mu A$.[10] These values are within the range of estimated values from the process parameters.

By changing the magnetic flux through the PC qubit, the depth of each well of the double-well potential changes, with one becoming deeper as the other becomes shallower. The energy bias (ε) is the energy difference between the minima of the two wells. (We will also use it to indicate the difference between energy levels in opposite wells, using a subscript to indicate which energy levels we are measuring the difference between.) It is periodic with frustration, f_q, which is the magnetic flux bias of the qubit in units of flux quanta. At $f_q = 0.5$, the depths of the two wells are equal, and near this value the energy bias varies almost linearly with frustration, such that ε is approximately $4\pi\alpha E_J(f_q - 0.5)$, where $E_J = I_c\Phi_0/2\pi$ is the Josephson energy of each of the two larger junctions of the qubit.

In our previous experiments,[10] we observed the rate of thermal activation of the qubit's phase particle (the term for the wave function of the qubit's phase) above the barrier between the two wells. At low temperatures, thermal activation is insufficient to overcome this barrier within the measurement time scale when $f_q = 0.5$. In this case, hysteresis is observed, where the PC qubit remains in the state in which it is prepared until it is measured, even though this state is no longer the minimum energy state. During the measurement, the SQUID goes to its voltage state, where it oscillates, and since its oscillations are strongly coupled to the qubit, the qubit is effectively randomized. Thus the hysteresis is not observable without preparing the qubit prior to each measurement. The qubit can be prepared in a state by changing its magnetic flux bias to a value where the system has a single well and allowing the qubit to relax to its ground state, then bringing it back to the magnetic flux bias where it is measured. The qubit will remain in the state where it was prepared, either the left well (the **0** state) or the right well (the **1** state), until either thermal activation or quantum tunneling provides the opportunity to escape to the opposite well.

III. ENERGY LEVEL STRUCTURE CALCULATIONS

The full Hamiltonian for the qubit in Fig. 1(a) is given in Eq. (1),

$$H = \frac{1}{2}C_j\left(\frac{\Phi_0}{2\pi}\right)^2\dot{\varphi}_1^2 + \frac{1}{2}C_j\left(\frac{\Phi_0}{2\pi}\right)^2\dot{\varphi}_2^2 + \frac{1}{2}\alpha C_j\left(\frac{\Phi_0}{2\pi}\right)^2\dot{\varphi}_3^2$$
$$+ E_J(1-\cos\varphi_1) + E_J(1-\cos\varphi_2) + \alpha E_J(1-\cos\varphi_3)$$
$$+ \left(\frac{\Phi_0}{2\pi}\right)^2\frac{(\varphi_1 - \varphi_2 + \varphi_3 + 2\pi f_q)^2}{2L_q}. \tag{1}$$

Here C_j is the junction capacitance of each of the larger junctions, and φ_i is the phase difference across junction i. If the inductance of the qubit is small enough, the phase of the three junctions is highly confined by flux quantization, and only two independent variables are necessary to describe the Hamiltonian. The requirement for this approximation is that $\beta_L = L_q/L_J < 0.01$,[13] where L_q is the inductance of the qubit loop and L_J is the Josephson inductance of each of the larger junctions. This is not the case in our sample, where $\beta_L = 0.1$. In order to correctly solve the Hamiltonian of our device, we need to include the inductance and solve for the three-dimensional Hamiltonian. We start by making a change of variables from the phases of the three junctions to Θ_1 and Θ_2, which are node phases, and I_m, which is the current around the PC qubit loop (we later use the variable I_p to denote the persistent current in the qubit, but I_p is technically the expectation variable in each state, while I_m is the quantum variable, thus $I_p = \langle I_m \rangle$). These variables are shown in Fig. 1(b). This gives us the equalities in Eq. (2) for converting the phase variables of the junctions into Θ_1, Θ_2, and I_m,

$$\varphi_1 = \Theta_1 - \left(\frac{1-b}{2}\right) 2\pi \left(\frac{L_q I_m}{\Phi_0} + f_q\right),$$

$$\varphi_2 = \Theta_2 + \left(\frac{1-b}{2}\right) 2\pi \left(\frac{L_q I_m}{\Phi_0} + f_q\right),$$

$$\varphi_3 = \Theta_2 - \Theta_1 - (b) 2\pi \left(\frac{L_q I_m}{\Phi_0} + f_q\right). \quad (2)$$

The variable b, which describes how the self-inductance of the qubit is divided among its branches, is arbitrary so long as it is less than 1. We can define its value as $1/(1 + 2\alpha)$ so that it eliminates any product terms of the time derivative of I_m and the time derivative of either Θ_1 or Θ_2 in the Hamiltonian. By changing variables again, this time to $\Theta_+ = (\Theta_1 + \Theta_2)/2$ and $\Theta_- = (\Theta_1 - \Theta_2)/2$, while defining the effective masses associated with these two variables as $M_+ = 2(\Phi_0/2\pi) 2C_j$ and $M_- = (2 + 4\alpha)(\Phi_0/2\pi) 2C_j$, we get the Hamiltonian in Eq. (3),

$$H = \frac{1}{2} M_+ \dot{\Theta}_+^2 + \frac{1}{2} M_- \dot{\Theta}_-^2 + \frac{\alpha}{2 + 4\alpha} C_j L_q^2 \dot{i}_m^2$$

$$+ E_J \left\{ 2 + \alpha - 2 \cos \Theta_+ \right.$$

$$\times \cos\left[\Theta_- - \left(\frac{1-b}{2}\right) 2\pi \left(\frac{L_q I_m}{\Phi_0} + f_q\right)\right]$$

$$\left. - \alpha \cos\left[-2\Theta_- - (b) 2\pi \left(\frac{L_q I_m}{\Phi_0} + f_q\right)\right] \right\}. \quad (3)$$

While complex, this is numerically solvable by discretizing the variables Θ_+, Θ_-, and I_m into Θ_{+_i}, Θ_{-_j}, and I_{m_k},
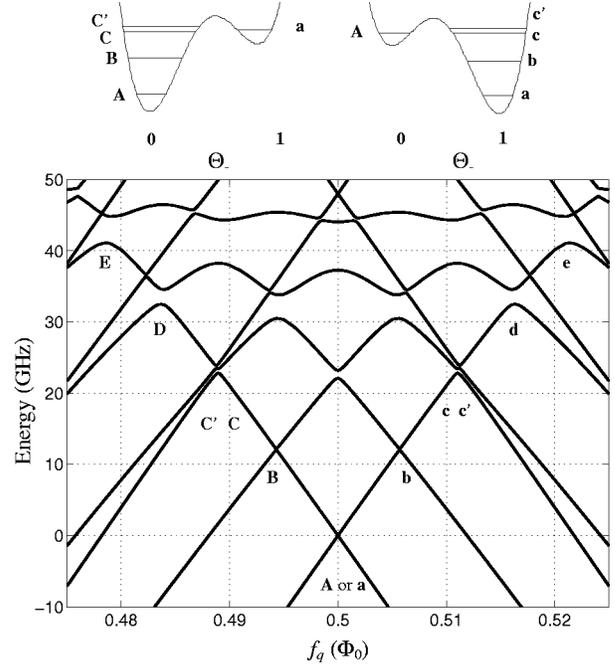
FIG. 2. An energy band diagram of the PC qubit with the parameters described in the text, with the magnetic flux bias of the qubit in units of flux quanta (f_q) as the horizontal axis. The transitions between the **0** and **1** states occur at the avoided level crossings. These are at $f_q = 0.478$, 0.483, 0.487, 0.488, 0.494, and 0.500 on the left side, labeled **E**, **D**, **C′**, **C**, **B**, and **A**, respectively. On the right side, these are at $f_q = 0.500$, 0.506, 0.512, 0.513, 0.517, and 0.522, labeled **a**, **b**, **c**, **c′**, **d**, and **e**. The energy levels in the double-well potential above the energy band diagram are likewise labeled. **C** in the energy band diagram comes from the alignment of **a** (in the right well) and **C** (in the left well), while **c** in the energy band diagram comes from the alignment of energy levels **A** and **c**. Since all the alignments are between a higher energy level in the deeper well and the lowest level in the shallow well, the avoided level crossings are designated by the label of the energy level in the deeper well.

respectively, and creating a Hamiltonian matrix whose elements are $H_{\mathbf{pq}} = \langle \Theta_{+_i} \Theta_{-_j} I_{m_k} | \hat{H} | \Theta_{+_r} \Theta_{-_s} I_{m_t} \rangle$, where **p** and **q** are indices that map onto all the permutations of **i**, **j**, **k** and **r**, **s**, **t**, respectively. H is a square matrix where each side has a length equal to the product of the number of discretized elements of Θ_+, Θ_-, and I_m. The matrix must be kept sparse in order to solve on a computer due to memory limitations, and the band structure in Fig. 2 shows the eigenvalues of this Hamiltonian matrix as the external magnetic flux bias is changed. The inclusion of self-inductance changes the energy band diagram, most significantly by reducing the level repulsion, since the barrier between the two wells is greater due to the need to overcome the qubit's self-inductance. The junction capacitance (C_j) is the most roughly estimated of the qubit's parameters, and thus serves as the sole fitting parameter for the level crossing locations. A value of 28 fF for C_j gives a good fit. The first six avoided crossings, counting outward from $f_q = 0.5$, are labeled, using **a**, **b**, **c**, **c′**, **d**, and **e** for the level crossings when f_q is greater than 0.5, and using **A**, **B**, **C**, **C′**, **D**, and **E** when f_q is less

than 0.5. **C** and **C**′ (and their equivalents in the other direction, **c** and **c**′) are difficult to discern due to their proximity. Although the energy scales are such that some of the avoided level crossings appear to actually cross in this figure, there is a small amount of energy level repulsion even at $f_q = 0.5$. There are multiple energy levels in each well, and each labeled level crossing corresponds to the alignment of the lowest level in one well and one of the energy levels in the other well, as is shown in the double well potentials in Fig. 2. This results in two eigenstates—a symmetric state and an antisymmetric state—spanning both wells, with an energy difference equal to the level splitting shown in the energy band diagram, allowing the classical state of the qubit to change as the phase particle oscillates between wells.

IV. RESULTS AND DISCUSSION

To determine the state of the PC qubit, we ramp the electrical current in the dc SQUID until it switches to the voltage state. The measuring dc SQUID remains in the zero-voltage state as long as the current through it is below the switching current, which is determined by the total magnetic flux through the SQUID; when it passes this current it develops a finite voltage. The nominal value of the switching current is $I_{sw0} = 2I_{c0}|\cos(\pi f'_S)|$, where I_{c0} is the critical current of each of the two SQUID junctions and f'_S is the total magnetic flux through the SQUID in units of flux quanta, although the SQUID may switch early due to thermal excitation or quantum tunneling of the SQUID phase particle. Since the qubit's two states have different magnetizations, the two states induce different switching currents in the SQUID: I_0 for state **0** and I_1 for state **1**. The stochastic process that describes the switching of the SQUID has a variance that is measurable but significantly smaller than the signal we are measuring (the difference between I_0 and I_1). The ramp rate is typically 4 μA/ms and the difference between I_0 and I_1 is 0.5 μA, which gives a delay of 125 μs between the polling of the **0** state and the **1** state. If the qubit is in the **0** state, the SQUID switches as soon as it arrives at I_0. If it is in the **1** state and remains there, the SQUID does not switch until it reaches I_1.

Figure 3 illustrates the observed hysteresis of the qubit. Part (a) of this figure shows the probability of measuring the qubit in each state by plotting $P_1 - P_0$, where P_1 is the probability of finding it in state **1** and P_0 is the probability of finding it in state **0**. It also shows one-dimensional cuts of the double-well potential at different magnetic fields. The solid curve is $P_1 - P_0$ when the system is prepared in the **1** state, while the dashed curve shows this measurement when it is prepared in the **0** state. This measurement occurs at ~20 mK bath temperature, where the thermal energy is $k_B T \approx 1.7$ μeV. Part (b) of this figure shows how the difference between the 50% point of the two curves shown in (a) (marked by the line labeled w) varies with temperature. We call this difference the "hysteresis width." The width is constant up to $T = 200$ mK, then decreases linearly as temperature increases. The hysteresis width should not vary with temperature as long as $k_B T < \hbar \omega_0$, where ω_0 is the resonant frequency of the qubit, which is equal to 28 GHz. This gives

(a)

(b)
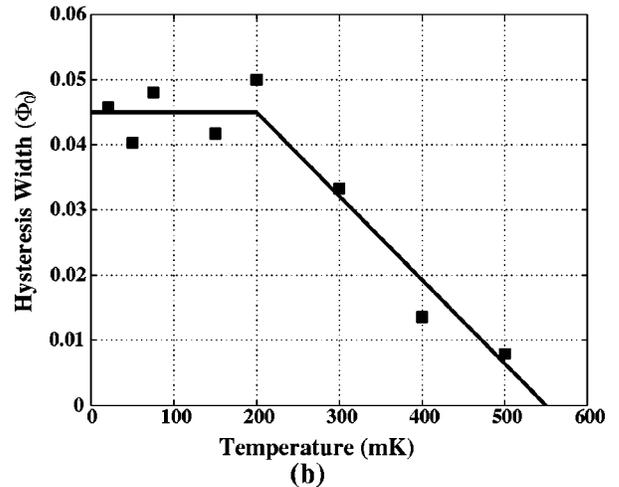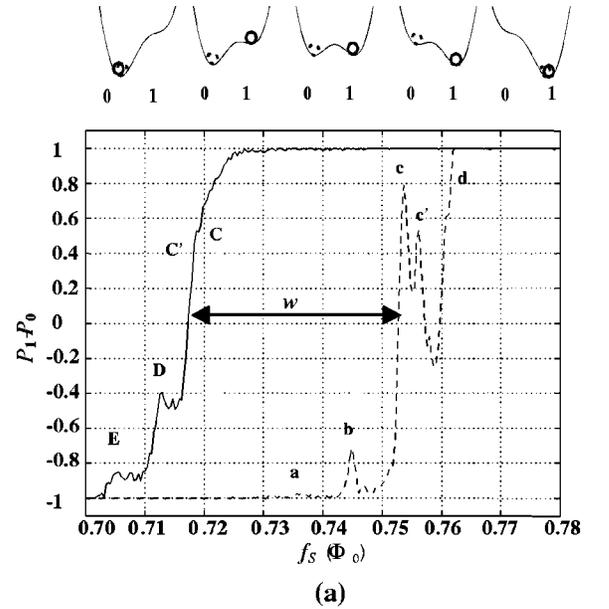
FIG. 3. (a) The hysteresis measurement at 20 mK bath temperature. Above the figure are one-dimensional cuts of the potential that show the shape of the double-well potential at the various frustrations. The plot shows the proportion of switching events where the qubit is measured in the **1** state minus the proportion where it is found in the **0** state ($P_1 - P_0$) against the magnetic flux bias of the dc SQUID in units of flux quanta (f_S). The solid line is for a qubit prepared in the **1** state, represented in the double-well diagrams as a solid circle. The dashed line shows the measured qubit state when it is prepared in the **0** state, corresponding to the dashed circle in the double-well potential diagrams. The dashed line shows numerous peaks and dips, while the solid line's structure is less pronounced. Multiple scans over the same region produce the same results. The width of the hysteresis is labeled in this figure with a w. (b) As the temperature increases, the hysteresis loop closes. The points on this graph show the width of the hysteresis loop (w) vs temperature. It is nearly constant for low temperatures and nearly linear for higher temperatures. The line serves as a guide for the eyes.

a turnover point of 210 mK, consistent with the measurement. Thermal activation causes the qubit to change state once the barrier is on the order of $k_B T$, and the barrier height

changes linearly with magnetic flux bias. The hysteresis width intercepts zero at 550 mK, or 47 μeV.

The hysteresis loop closes as the temperature increases. The hysteresis width corresponds to the points where the probability of escape from the shallow well is approximately 50%, or $P_{esc} = 1 - e^{-\Gamma_{th}t} = 0.5$. Since the ramp time is on the order of 1 ms, we can calculate Γ_{th} to be approximately 700. Thermal activation gives an escape rate of $\Gamma_{th} = (7.2\Delta U\omega_0/2\pi Qk_BT)\exp(-\Delta U/k_BT)$. Calculations of the potential energy, confirmed by previous experiments, show how the barrier between the two states, ΔU, varies with the magnetic flux bias of the qubit.[10] Near $f_q = 0.5$, the barrier for the qubit to make the transition from the **1** to the **0** state can be written as $\Delta U_{10}(f_q) \approx \Delta U(0.5) + 2\pi\alpha E_J(f_q - 0.5)$, where $2\pi\alpha E_J = 9500$ μeV. $\Delta U(f_q = 0.5)$ is $2\pi\alpha E_J\{2\cos^{-1}[2\sqrt{(1-\alpha)^2/3}] - \cos^{-1}[\sqrt{(1-\alpha)^2/3\alpha^2}]\}$, or about 210 μeV,[10] or 2.4 K. $\Delta U_{01}(f_q) \approx \Delta U(0.5) - 2\pi\alpha E_J(f_q - 0.5)$ is the barrier for the transition from **0** and **1** at the same flux bias. $\Delta U(f_q)/k_BT$, which appears in both the exponent and the prefactor, is the dominant term in Γ_{th}. The other terms in the prefactor are ω_0, the simple harmonic-oscillator frequency of the well (equal to 28 GHz), and the quality factor Q, which is 3×10^5 as calculated in Ref. 10. The value of $\Delta U(f_q)/k_BT$, which would give a Γ_{th} of 700, is 9. Referring to part (b) of Fig. 3, we can apply the values of the temperature and the barrier of the shallow well, $\Delta U(f_q)$, to the slope of the line to find the constant value of $\Delta U(f_q)/k_BT$, which is found to be 7.3, about 20% off from the theoretical value of 9.

Figure 4 shows the number of switching events at various values of current and magnetic flux bias. The horizontal axis represents the externally applied magnetic flux to the SQUID in terms of frustration, while the vertical axis corresponds to the current bias of the SQUID. The coloring indicates the number of switching events that occur at each point in the external flux bias and current bias coordinates. In the experiment, 10^3 measurements are taken at each value of external flux bias, so each vertical slice represents a histogram of these measurements. Over most of the parameter space, this figure shows that two preferred states exist, corresponding to the **1** and **0** states of the qubit. These states create two "lines" across the figure, reminiscent of the results in Ref. 14.

However, the detailed signatures of the switching events when the qubit is prepared in the **1** state [Fig. 4(a)] differ from when it is prepared in the **0** state [Fig. 4(b)], even though the energy biases are mirror images of each other around $f_q = 0.5$, as shown by the double-well potentials drawn above Fig. 3(a). Figure 4(a) shows stripes in the region in between the two lines of switching currents, whereas Fig. 4(b) has no switching events in this in-between region. The two lines of switching currents in Fig. 4(b) shows island-like regions, whereas Fig. 4(a) does not. The plots in Fig. 3, which are derived from the same data, also reflect this asymmetry. Although Figs. 4(a) and 4(b) show a range of flux bias where both states can be measured, an important difference between the two plots is the path followed by the SQUID in bias current and external magnetic field, which is illustrated by the dashed line in the two figures. Rather than

(a)

(b)
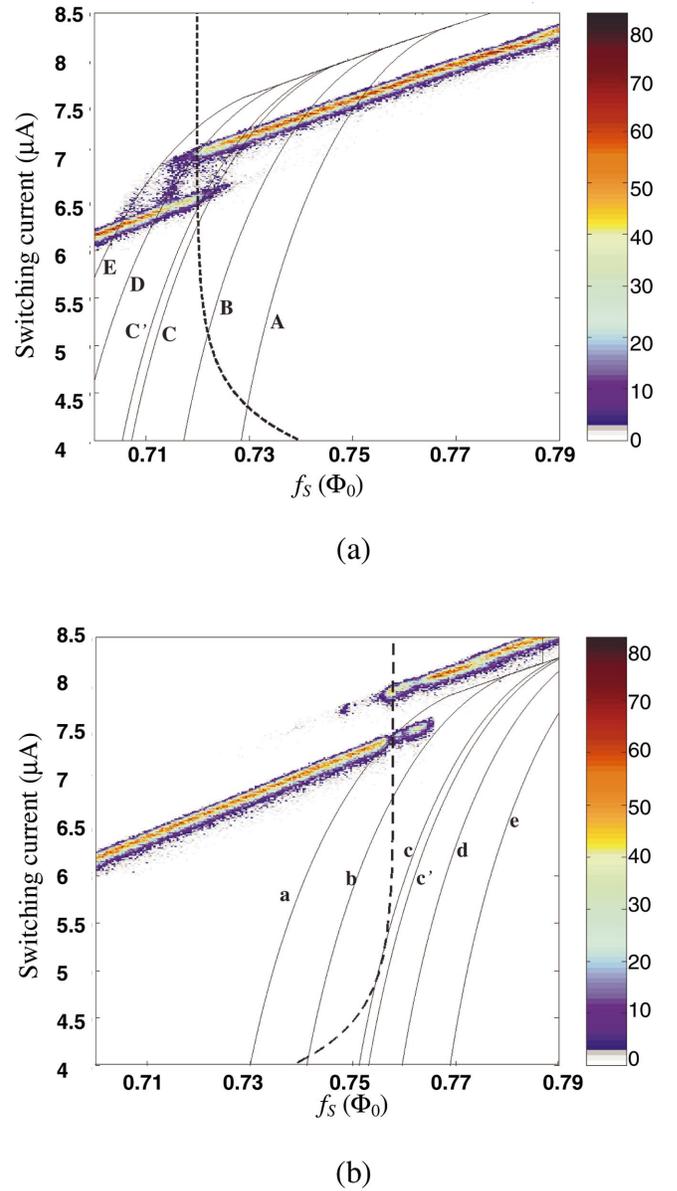
FIG. 4. (Color) (a) A plot of the switching events at various external flux biases when the qubit is prepared in the **1** state, taken at 20 mK bath temperature. Each vertical slice is a histogram of an ensemble of switching measurements taken at a fixed external flux bias, where the colors represent the number of switching events at each current bias. The horizontal axis is the external flux bias of the SQUID, f_S. The solid lines are lines of constant f_q that correspond to level crossings in the qubit labeled according to the convention in Fig. 2. The path followed when the current bias of the SQUID is ramped is not a straight vertical line, since the external flux bias is also changing due to the state preparation. The path for a representative measurement, where $f_S = 0.72$, is shown by the dashed line. (b) The switching events when the qubit is prepared in the **0** state, also at 20 mK. Note that the dashed line is briefly tangential with one of the solid lines. The dashed line represents $f_S = 0.753$.

being completely vertical, indicating a ramp in SQUID current while the external magnetic field is held constant, the external magnetic field also changes during the current ramp due to the preparation of the qubit state. The total magnetic

field seen by the qubit also changes due to coupling from the SQUID's circulating current. These, along with the influence of the time-ordered measurements, result in differences in the data due to macroscopic quantum tunneling.

We first consider the data in Fig. 4(a), where the system is initially prepared in the **1** state. When the qubit is prepared in the **1** state, it will remain there as long as the bias is such that the local minimum exists, unless it has some mechanism to escape this local minimum, such as thermal activation or macroscopic quantum tunneling. At 20 mK bath temperature, thermal activation is effectively frozen out, and macroscopic quantum tunneling is the dominant process; therefore, one expects to see tunneling at the locations of the energy level crossings on the left side of the band diagram in Fig. 2. The probability that the state will make a transition from **1** to **0** depends on the tunneling rate and the time that the system remains in the level-crossing region. Note that if the qubit makes the transition to the **0** state before the SQUID bias current reaches I_1 but after the current is past I_0, the SQUID switches immediately, and we record a switching event in the region between I_0 and I_1. One might expect vertical stripes to appear between I_0 and I_1 at the external flux biases corresponding to the level crossings. The observed stripes are instead curved because the total flux bias of the qubit, f_q, depends on the flux coupled from the readout SQUID as well as the externally applied flux, f_q^{ext}. The total flux biasing the qubit is $f_q = f_q^{ext} + MI_{cir}/\Phi_0$, where f_q^{ext} is the externally applied flux bias, M is the mutual inductance between the dc SQUID and the qubit, and I_{cir} is the circulating current in the SQUID. The circulating current in the dc SQUID decreases as the bias current increases. The circulating current is calculated from the Josephson equations of a SQUID with a finite self-inductance to be $I_{cir} = I_{c0}\sin(\pi f_S')\sqrt{1 - I_{bias}^2/[2I_{c0}\cos(\pi f_S')]^2}$, where f_S' is the effective flux bias of the SQUID, which follows the equation $f_S' = f_S + MI_p/\Phi_0 + L_S I_{cir}/\Phi_0$. Here f_S is the externally applied flux bias to the dc SQUID and L_S is the self-inductance of the SQUID. I_p is the persistent current in the qubit, which is nearly constant at $\alpha I_c = 760$ nA, and whose sign depends on the state in which the qubit is prepared. The appearance of I_{cir} in f_S' requires that the circulating current be solved self-consistently. This calculation shows that the qubit's effective flux bias approaches the externally applied flux as it moves closer to the switching current. Figure 5 shows how f_q changes as the current is ramped. Lines of constant effective flux bias are drawn in Fig. 4(a) and the stripes in the switching events match up with these lines of constant f_q. Furthermore, the lines of f_q that match up to the stripes indicate the effective flux biases where the level crossings occur in the qubit, and these stripes compare well to the calculated level crossings of the qubit (shown in Fig. 2) based on the parameters we obtained from thermal activation experiments.[15] By ramping the bias current more slowly, the system spends more time near the level crossings that have a smaller tunneling rate and they show up more clearly; in this way, all the level crossings have been mapped out and show all the expected energy levels.[16] The effect of the ramp rate is discussed further below.
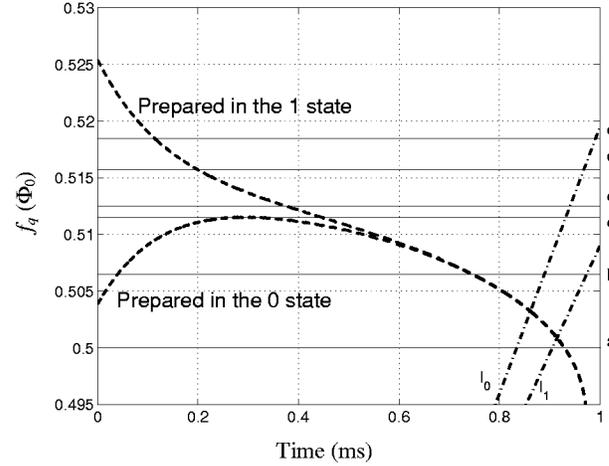
FIG. 5. The trajectory followed by f_q during the SQUID bias current ramp when $f_S = 0.753$ ($f_S = 0.753$ would correspond to $f_q = 0.469$ if the qubit were not influenced by the circulating current in the SQUID). The solid lines are level crossings of the qubit (labeled according to the convention in Fig. 2), while the dashed lines are the paths followed when the qubit is prepared in the **0** state and in the **1** state. The plateau that occurs when the qubit is prepared in the **0** state causes sharp peaks in the data due to the time during which the qubit flux bias lingers at a level crossing. The dashed-dotted lines are the times at which the switching currents for states **0** and **1** are reached for each value of f_q.

We now consider the data in Fig. 4(b), where the qubit is initially prepared in the **0** state. If the qubit remains in the **0** state, then the SQUID switches to the voltage state at I_0. The qubit cannot change from the **0** state to the **1** state after I_0, since by that point the SQUID will already have switched. If there is a transition from **0** to **1**, this must happen before the qubit reaches I_0. There are no observed switching events when the current bias is between I_0 and I_1, indicating that once it makes the transition from **0** to **1** it does not return. This is expected if after tunneling into one of the higher energy levels of the deeper well, it relaxes to a lower energy state where it is no longer in alignment with the energy level of the shallow well. Figure 6(a) shows the same data as Fig. 4(b), but simplified to the probability of finding the qubit in each state, $P_1 - P_0$. The large population shift in Fig. 4(b) at $f_S = 0.755$ is represented in Fig. 6(a) by the peak labeled **c**. Slowing down the measurement has a noticeable effect when the qubit is prepared in the **0** state, shown by how the peaks grow larger from part (a) to (b) while maintaining their position, indicating that the probability of transition grows due to the slowing of the SQUID ramp rate. This suggests that the tunneling rate from the **0** to **1** state is comparable to the time over which the levels are near alignment in the SQUID ramp. If the rate were much faster, then all the population would tunnel to the **1** state. If it were much slower, then none of the population would tunnel.

Recall that the flux bias of the qubit is $f_q = f_q^{ext} + MI_{cir}/\Phi_0$. Since I_{cir} changes as the SQUID is ramped, and f_q^{ext} is pulsed when the qubit is prepared, f_q is a function of time. In the qubit's preparation, the external magnetic field is pulsed in either the positive direction (to prepare it in the **1**
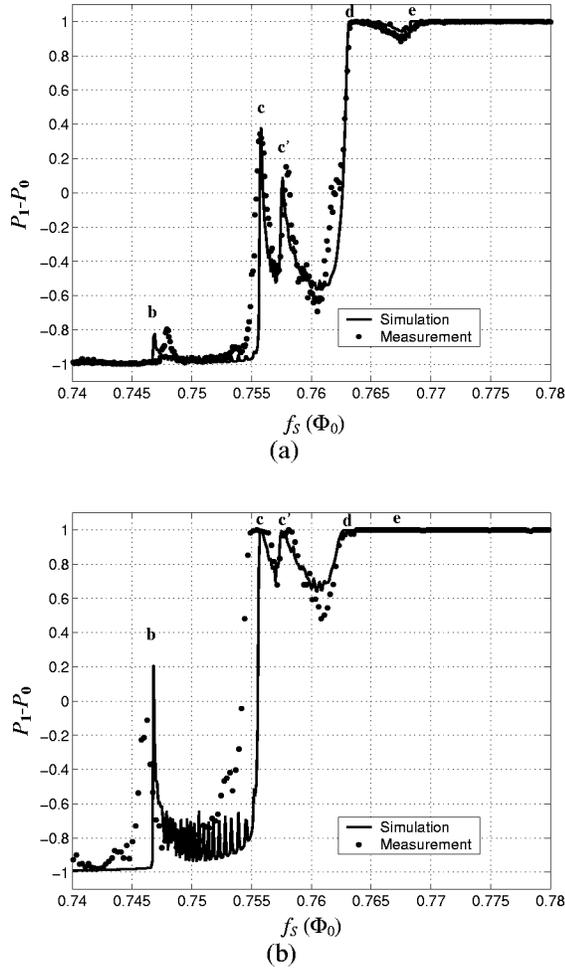
FIG. 6. The qubit state when the SQUID is ramped at a rate of (a) 4 μA/ms and (b) 0.8 μA/ms. The solid lines correspond to the theoretical model, while the solid circles are actual data points. The two show reasonably good agreement. The slower ramp rate results in a higher probability that the qubit will move to the **1** state, as is made clear by the growing peaks. The oscillations in (b) between $f_S = 0.748$ and 0.755 are artifacts of the numerical simulation. They decrease as resolution is increased, but resolution is limited by computer memory constraints. The peak labels correspond to the avoided crossings indicated in Fig. 2.

well) or the negative direction (to prepare it in the **0** well). It returns from the preparation while the SQUID's bias current is ramping. The change in I_{cir} during the SQUID ramp is the same regardless of the well in which the qubit is prepared. Thus, when the qubit is prepared in the **1** state, the two factors sum, while preparation in the **0** state causes the two factors to oppose one another. In the case of preparation in the **0** state, the state preparation and the MI_{cir} magnetic fields balance for roughly 50 μs, where the flux bias of the qubit is nearly constant. This is seen in Fig. 5. When prepared in the **1** state, the curve shows a continuous change in f_q, while f_q plateaus briefly when the qubit is prepared in the **0** state. If this plateau corresponds to an energy bias where there is a high rate of quantum tunneling between the wells, this results in a strong probability of tunneling which gives a sharp peak in the measured data ($P_1 - P_0$).

V. SIMULATIONS OF TRANSITIONS

To simulate the effect of the SQUID current bias ramp on the state of the qubit, an equation for the tunneling rate is needed. These measurements resemble those taken in Ref. 3 and described theoretically in Ref. 17 to give an equation for the rate of transition from the lowest energy level in one well to a high energy level in the other,

$$\tau_i^{-1} = \frac{\Delta_i^2 \Gamma_i}{2\Delta_i^2 + \Gamma_i^2 + 4\varepsilon_i^2}, \tag{4}$$

where τ_i^{-1} is the transition rate for level crossing i, Δ_i and ε_i are the tunnel splitting and energy bias of the specific level crossing, respectively, and Γ_i is the rate at which the qubit relaxes from the high energy level in the deeper well to one of the lower energy levels. The transition is not considered complete without this decay, which prevents the phase particle from returning to the original state. Δ_i is a function of the quantum model of the qubit, and can be calculated from the parameters that we already know. ε_i, the energy bias, is the energy difference between the energy levels in either well. This is equal to $4\pi\alpha E_J(f_q - f_i)$, where f_i is the position, in magnetic flux bias, of the individual level crossing we are considering. We will approximate Γ_i to be a constant for each level crossing. This relaxation to the lower energy levels is the fitting parameter, with the guideline that the higher the energy level, the more quickly it should relax. Running a simulation of the transition probability as f_q changes during the SQUID current bias ramp gives Figs. 6(a) and 6(b), showing a match between the theoretical model and the experiment at two different ramp rates. Using this model with theoretically calculated numbers for Δ_i, the fitted values for Γ_i are $(13 \ \mu s)^{-1}$ for the first excited state, $(15 \ \mu s)^{-1}$ for the second, $(75 \ \mu s)^{-1}$ for the third [which corresponds to a transverse mode of the oscillator and is weakly coupled to the other energy levels], $(1 \ \mu s)^{-1}$ for the fourth, and $(1 \ \mu s)^{-1}$ for the fifth. These are long decay times for intrawell relaxation. Recent spectroscopy data also suggest an intrawell relaxation time on the other of tens of microseconds.[18] It should be noted that the theory allows some trade-off between Δ_i and Γ_i, so that a smaller Δ would correspond to a faster relaxation time. Environmental fluctuations may effectively decrease Δ_i while increasing Γ_i, implementing this trade-off. While we modeled this reduction in Δ_i using Wilhelm's formulation,[19] the exact amount is necessarily uncertain since it depends on the total environment of the qubit, which we cannot directly observe.

There are several strong peaks in these data, including two that are right next to each other. In the quantum model of the qubit, the only point that would give two level crossings so close together would be due to a transverse mode of the three-dimensional well, which produces an energy level of the first excited state in the Θ_+ direction near the energy level as the second excited state in the Θ_- direction. We presume that we are able to observe this mode only because of an asymmetry in the two larger junctions, due to fabrication variances, since perfectly symmetric junctions would
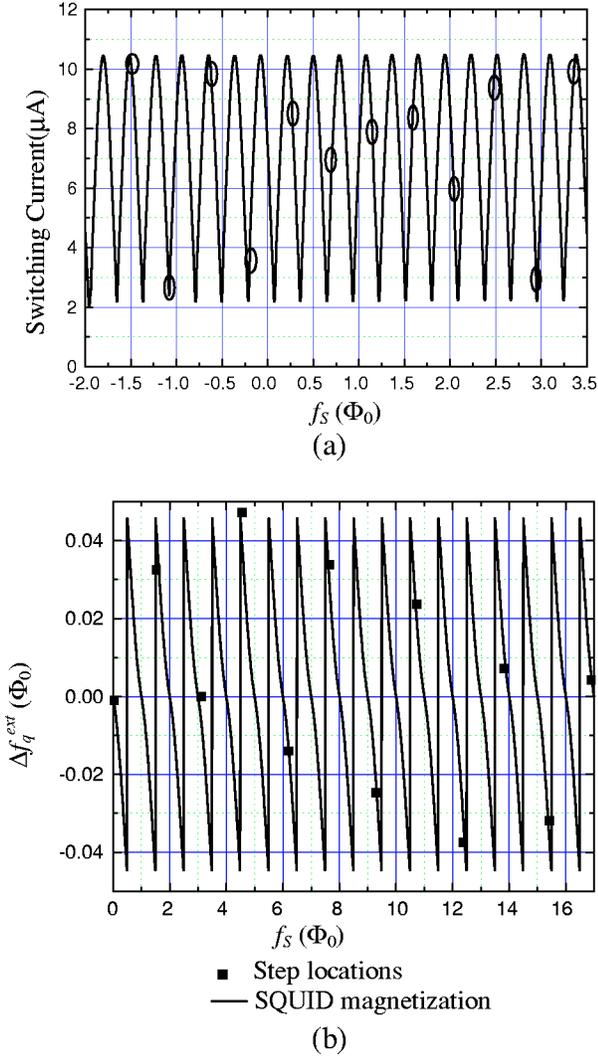
FIG. 7. (a) This is the dc SQUID switching current curve, which approximately follows $I_{sw0} = 2I_{c0}|\cos(\pi f'_S)|$. The locations of the qubit steps are circled. The dc SQUID switching current is periodic with magnetic field, while the qubit step is nearly periodic. (b) The solid squares represent the deviations of the measured qubit step locations from a perfect periodicity of 1.53 SQUID periods per qubit period, while the solid line shows the magnetic field from the SQUID's circulating current which couples to the qubit. This is periodic with the SQUID's frustration, and accounts for the deviations from perfect periodicity.

not produce a coupling between the transverse mode energy level in the deep well and the lowest state in the shallow well.

Using data from preparation in both states, we have observed energy levels within each well, which are separated from the ground state by frequencies of 28, 53, 60, and 72 GHz. This is measured from the location of the stripes when prepared in the **1** state and the location of the peaks when prepared in the **0** state, using the estimation that $\varepsilon \approx 4\pi\alpha E_J(f_q - 0.5)$. The locations of these level crossings agree well with the energy band diagram in Fig. 2, which is calculated by numerically finding the eigenstates of the Hamiltonian.

VI. SUMMARY

In summary, we have observed macroscopic quantum tunneling in a persistent current qubit. The observed stripes when the qubit is prepared in the **1** state, even more than the distinct variations in the state populations when it is prepared in the **0** state, indicate quantum level crossings of states in the qubit's wells. We used these observed stripes and variations to determine E_C, our only unknown parameter after the results in Ref. 10, so that the quantum simulation gives the same crossings as those measurements. Once the location of the level crossings was determined, the probability of tunneling led to an estimate of the intrawell relaxation times in the tens of microseconds. Experiments are underway to observe coherent oscillations between the states.

APPENDIX:

Calculating the mutual inductance between the dc SQUID and the qubit is straightforward. The self-inductance of the SQUID can be determined from the transfer function of magnetic flux to switching current. From these values, we can calculate the circulating current in the SQUID as it varies with frustration. The shape of this curve, especially its minimum and any bimodal features due to multiple wells in its potential, tells us the value of $\beta_{L,S} = L_S/L_{J,S}$, the ratio of the SQUID's self-inductance to its Josephson inductance. Figure 7(a) shows the periodicity with which the qubit step appears in the SQUID transfer function. Since the SQUID is 1.53 times the size of the qubit, the step should appear at every 1.53 periods in the SQUID curve. This periodicity arises because, while both the SQUID and the qubit have a periodicity of Φ_0, the SQUID receives more flux due to its larger size. However, the qubit is not perfectly periodic, as is shown in Fig. 7(b), where the points mark Δf_q^{ext}, the difference between the qubit step's position and where it would appear if it occurred with perfect periodicity. This deviation indicates that there are sources of magnetic field other than that applied by the external magnet, the strongest of which is the field coupled to the qubit by the circulating current in the dc SQUID. (The SQUID is also influenced by the circulating current in the qubit, but since this is only one-seventh of the value of the circulating current in the SQUID, it can be

safely neglected.) The total field seen by the qubit is $f_q = f_S/1.53 + MI_{cir}/\Phi_0$, where f_S is the frustration of the SQUID from the externally applied field and I_{cir} is the circulating current in the SQUID. Thus $\Delta f_q^{ext} = f_q - f_S/1.53$ $= MI_{cir}/\Phi_0$. If we use a least-squares fit to find a value of M that causes MI_{cir}/Φ_0 to intersect the Δf_q^{ext} data points, we can solve for M, which we find to be about 25 pH. This produces the curve in Fig. 7(b) that intersects the data points.

[1] A. J. Leggett and A. Garg, Phys. Rev. Lett. **54**, 857 (1985).

[2] S. Lloyd, Science **261**, 1569 (1993).

[3] R. Rouse, S. Han, and J. E. Lukens, Phys. Rev. Lett. **75**, 1614 (1995).

[4] J. R. Friedman, V. Patel, W. Chen, S. K. Tolpygo, and J. E. Lukens, Nature (London) **406**, 43 (2000).

[5] C. H. van der Wal, A. C. J. ter Haar, F. K. Wilhelm, R. N. Schouten, C. J. P. M. Harmans, T. P. Orlando, S. Lloyd, and J. E. Mooij, Science **290**, 773 (2000).

[6] Y. Nakamura, Y. A. Pashkin, and J. S. Tsai, Nature (London) **398**, 786 (1999).

[7] J. M. Martinis, S. Nam, J. Aumentado, and C. Urbina, Phys. Rev. Lett. **89**, 117901 (2002).

[8] Y. Yu, S. Han, X. Chu, S. Chu, and Z. Wang, Science **296**, 889 (2002).

[9] J. E. Mooij, T. P. Orlando, L. Levitov, L. Tian, C. H. van der Wal, and S. Lloyd, Science **285**, 1036 (1999).

[10] K. Segall, D. Crankshaw, D. Nakada, T. P. Orlando, L. S. Levitov, S. Lloyd, N. Markovic, S. O. Valenzuela, M. Tinkham, and K. K. Berggren, Phys. Rev. B **67**, 220506 (2003).

[11] K. K. Berggren, E. M. Macedo, E. M. Feld, and J. P. Sage, IEEE Trans. Appl. Supercond. **9**, 3271 (1999).

[12] M. Kamon, M. J. Tsuk, and J. K. White, IEEE Trans. Microwave Theory Tech. **42**, 1750 (1994).

[13] D. S. Crankshaw and T. P. Orlando, IEEE Trans. Appl. Supercond. **11**, 1006 (2000).

[14] H. Takayanagi, H. Tanaka, S. Saito, and H. Nakano, Phys. Scr., T **T102**, 95 (2002).

[15] While Ref. 10 accurately gave us the values of E_J, α, and Q, the value of E_C was not as well determined. These measurements show us the location of the level crossings in Fig. 4(a). We can determine the value of E_C that gives these energy biases for the level crossings, which we find to be 3 μeV, also giving us C_j as 28 fF.

[16] D. S. Crankshaw, Ph.D. thesis, MIT (2003).

[17] D. V. Averin, J. R. Friedman, and J. E. Lukens, Phys. Rev. B **62**, 11 802 (2000).

[18] Y. Yu, D. Nakada, Janice C.Lee, Bhuwan Singh, D. S. Crankshaw, T. P. Orlando, K. K. Berggren, and W. D. Oliver, Phys. Rev. Lett. **92**, 117904 (2004).

[19] F. K. Wilhelm, Phys. Rev. B **68**, 060503 (2003).